Indentation-induced microhardness and dielectric studies of flux-grown gadolinium aluminate crystals

1998 J. Phys.: Condens. Matter 10 5277

(http://iopscience.iop.org/0953-8984/10/24/006)

J. Phys.: Condens. Matter **10** (1998) 5277–5287. Printed in the UK PII: S0953-8984(98)87383-9

Indentation-induced microhardness and dielectric studies of flux-grown gadolinium aluminate crystals

K K Sharma†, P N Kotru†, R P Tandon‡ and B M Wanklyn§

† Department of Physics, University of Jammu, Jammu, India
‡ National Physical Laboratory, New Delhi, India
§ Clarendon Laboratory, University of Oxford, Oxford, UK

Received 8 September 1997, in final form 29 January 1998

Abstract. Results of microhardness measurements and dielectric studies carried out on flux-grown $GdAlO_3$ single crystals are presented. Load independent values of hardness are estimated for (110) and (001) planes by applying the law of Hays and Kendall. The values of fracture toughness and brittleness index are calculated for median cracks at higher loads. Hardness anisotropy for both the crystal planes considered is reported. The dielectric constant, dielectric loss and conductivity are found to be dependent on temperature as well as frequency of the applied a.c. field. The anomalous behaviour of dielectric constant against temperature suggests some transition taking place at 170 °C.

1. Introduction

Indentation-induced hardness testing studies provide useful information concerning the mechanical behaviour of different materials. A systematic study of the Vickers microhardness of gadolinium aluminate was undertaken with the aim of investigating the dependence of microhardness on applied load and also to study its fracture mechanics and hardness anisotropy.

A large number of simple or complex dielectric compounds of different structural families (single crystals, ceramics or thin film form) have been studied for understanding of their dielectric/ferroelectric characteristics. Perovskite structures, in general, are interesting materials for dielectric studies. Rare-earth orthoferrites, orthochromites and aluminates have in common a structure which is only slightly distorted from the perfect cubic perovskite. These materials are of interest on account of their magnetic, optical [1, 2] and dielectric properties. Lanthanium aluminate with low dielectric constant and low tangent loss has been proposed to be one of the most desirable substrates for the thin films of high-T_c superconducting materials [3]. Dielectric behaviour of $LaAlO_3$ powder has also been reported [4].

To the best of our knowledge, no results regarding the fracture mechanics and dielectric studies of $GdAlO_3$ have been reported. Kotru *et al* [5] have carried out microhardness measurements on pure, doped and mixed rare-earth aluminate crystals including $GdAlO_3$ and determined the microhardness value without giving reference to any particular plane. The present investigation reports microhardness testing on two different planes, (110) and (001) of $GdAlO_3$. In addition, the present study also discusses the directional variation of hardness and indentation-induced crack propagation, thereby giving the values of fracture toughness and brittleness index. Dielectric characteristics of the crystals are also reported.

0953-8984/98/245277+11$19.50

2. Experiment

2.1. Sample preparation

Large single crystals of $GdAlO_3$ were grown using $PbO/PbF_2/B_2O_3$ flux according to the procedure reported by Wanklyn [6]. The addition of B_2O_3 to the PbO/PbF_2 mixture resulted in a great improvement in crystal quality and size and twinning was greatly reduced. The major faces developed during growth in these crystals are (110) and (001) planes [7].

2.2. Indentation tests

Smooth and clean surfaces of the crystals were subjected to static indentation tests at room temperature using a Vickers microhardness tester (mhp-100) attached to an incident light microscope (Neophot-2). Loads ranging from 10 to 100 g (0.09–0.98 N) were used for making indentations, keeping time of indentation constant at 10 s in all cases. At least five indentation marks were obtained on each face for the same load, the distance between consecutive marks being kept more than three times the diagonal length of the indentation mark. The diagonal lengths of the indentation marks and crack lengths were measured using the micrometer eye-piece at a magnification of $\times 400$. The microhardness value was calculated using the equation [8],

$$H_v = 1.8544P/d^2 \text{ kg mm}^{-2} \tag{1}$$

where H_v is the Vickers hardness number, P is the applied load and d is the average diagonal length of the indentation mark.

2.3. Experimental error

The experimental error of the measurements of load P and diagonal length d of the indentation mark have been calculated for each value of H_v, using the relation:

$$\Delta H_v = 1.8544[(1/y\Delta P)^2 + P^2/y^4(\Delta y)^2]^{1/2}$$

where $y = d^2$ and $\Delta y = 2d\Delta d$; ΔP, Δy and Δd being errors in P, y and d respectively.

2.4. Dielectric measurements

For dielectric measurements, good quality crystals of $GdAlO_3$ having regular faces were selected. Silver paint was applied on both the opposite (110) faces to act as electrodes. The specimen was then mounted in a specially designed sample holder. The sample holder was placed in a furnace whose temperature was monitored using a platinum–rhodium thermocouple and Eurotherm temperature indicator.

The dielectric measurements were carried out using a fully automatic 4192 A impedance analyser (Hewlett Packard, USA) in the frequency range of 1 kHz to 13 MHz and temperature range of 20 to 210 °C. The values of capacitance C and dielectric loss ($\tan\delta$) could be read directly from the two display panels of the instrument. Knowing the values of capacitance, dielectric constant ϵ' was calculated using the relation

$$\epsilon' = Ct/8.85 \times 10^{-12} \text{ A} \tag{2}$$

where C, t and A represent capacitance, sample thickness and area of the crystal face respectively.

Using the values of dielectric constant ϵ' and dielectric loss ($\tan\delta$), the values of conductivity σ were calculated with the help of the following relation

$$\sigma = \omega_0 \epsilon_0 \epsilon' \tan\delta \tag{3}$$

where $\epsilon_0 = 8.85 \times 10^{-12}$ F m^{-1}, $\omega_0 = 2\pi f$, f being the frequency in hertz.

3. Results and discussion

3.1. Load dependence of hardness

The results presented in figure 1 show that the Vickers hardness number H_v decreases with load non-linearly up to a load of 0.7 N. after which it almost attains a saturation value. This behaviour can be qualitatively explained on the basis of the depth of penetration of the indenter. At small loads, the indenter penetrates only surface layers and the effect is more pronounced at these loads. However, as the depth of penetration increases, the effect of inner layers becomes more prominent and ultimately there is no change in the value of hardness with load [9]. This explanation is also favoured by Brookes [10], who associated the increase in hardness with the early stages of plastic deformation.

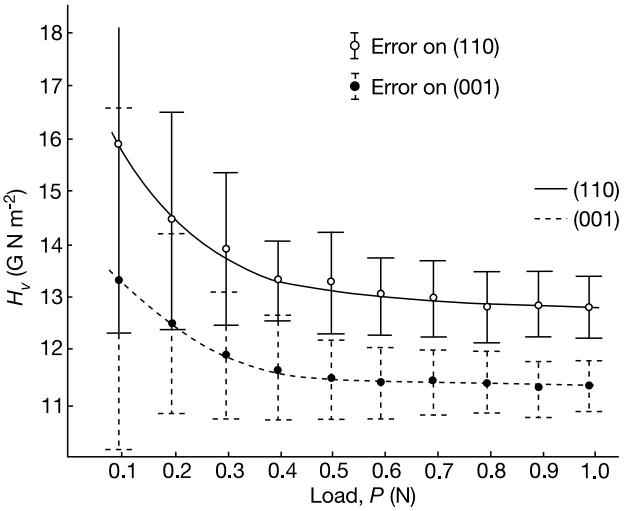

Figure 1. Graph showing dependence of Vickers hardness number H_v on applied load for (110) and (001) planes.

The non-linear behaviour of hardness with load is also observed in other aluminates [5] and can be mathematically explained by the law of Hays and Kendall, which is a slight modification of Kick's law. Kick [11] gave a relation between load P and diagonal length d of the indentation mark as

$$P = k_1 d^n \tag{4}$$

where k_1 is the standard hardness constant and n is the Meyer index which is proposed to be equal to 2. However, for the present crystal, the value of n was found to be less than 2 for both (110) and (001) planes. This discrepancy can be further explained by using the law of Hays and Kendall [12], according to which

$$P - W = k_2 d^2 \tag{5}$$

where W is the sample's resistance pressure and represents the minimum applied load to produce an indentation. The data on n, k_1, k_2 and W obtained through graphical methods as explained in the literature [5] are given in table 1. A logarithmic plot of (5), $\log(P - W)$ versus $\log d$, gives the value of $n = 2$ (figure 2), thus confirming the validity of the law of Hays and Kendall as applied to $GdAlO_3$ single crystals.

Table 1. Results of microhardness analysis.

Plane	H_v (GN m^{-2})	n	k_1 (GN m^{-2})	k_2 (GN m^{-2})	W/k_1 ($\times 10^{-12}$ m^2)	W (N)
(110)	13.59	1.80	10.98	6.59	2.92	0.032
(001)	11.83	1.88	8.18	5.97	2.42	0.019

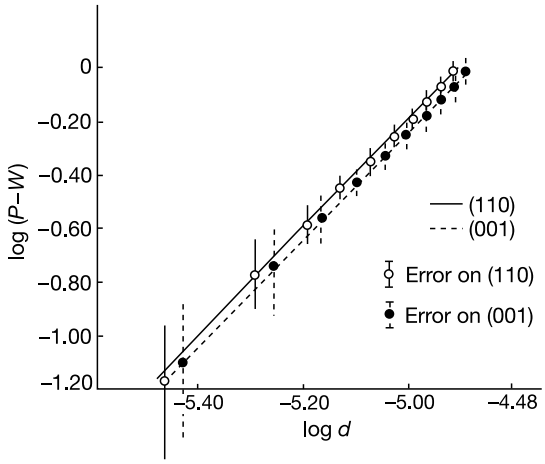

Figure 2. Graph of $\log(P - W)$ versus $\log d$ for the two planes.

Thus replacing P by $(P - W)$ in (1), we can write

$$H_v = 1.8544(P - W)/d^2. \tag{6}$$

Substituting for $(P - W)$ from (5), (6) yields

$$H_v = 1.8544k_2 \tag{7}$$

which gives the load independent values of H_v of (110) and (001) planes as

$$H_v(110) = 12.23 \text{ GN m}^{-2}$$
$$H_v(001) = 11.08 \text{ GN m}^{-2}.$$

3.2. Fracture mechanics

The indentation impressions are seen associated with cracks at all loads, whether the plane considered is (110) or (001). From table 2, it is clear that for both (110) and (001) planes of $GdAlO_3$ crystals, transition from Palmqvist to median cracks occurs at around 0.8 N load. For $c/a \geqslant 2.5$ (where a is half the diagonal length of the indentation mark), cracks formed

Table 2. Transition from Palmqvist to median cracks.

	(110)			(001)			
P (N)	c/a	K_c (MN m$^{-3/2}$)	B_i ($\times 10^3$ m$^{-1/2}$)	c/a	K_c (MN m$^{-3/2}$)	B_i ($\times 10^3$ m$^{-1/2}$)	Nature of cracks
0.098	2.07	—	—	2.03	—	—	Palmqvist
0.196	2.00	—	—	1.67	—	—	Palmqvist
0.294	2.08	—	—	1.63	—	—	Palmqvist
0.392	2.13	—	—	1.69	—	—	Palmqvist
0.490	2.18	—	—	1.72	—	—	Palmqvist
0.588	2.30	—	—	1.74	—	—	Palmqvist
0.686	2.40	—	—	2.09	—	—	Palmqvist
0.784	2.61	2.23	5.75	2.51	2.10	5.44	Median
0.882	2.75	2.05	6.26	2.75	1.87	6.04	Median
0.980	2.95	1.91	6.74	3.05	1.65	6.87	Median

around the indentation mark take the form of median cracks [13] and satisfactory value of fracture toughness K_c is obtained by using the following relation of Lawn and Fuller [14]

$$K_c = P/\beta c^{3/2} \tag{8}$$

where β is the indenter constant taken as 7 for the Vickers indenter. The average values of fracture toughness as calculated for median cracks come out to be 2.06 and 1.87 MN m$^{-3/2}$ for (110) and (001) planes respectively.

Figure 3 shows the variation of crack length with loads which increases for both the faces. Since with increase in load, hardness decreases, increase in crack length with load is attributed to decreases in hardness value. It may be noted that the linearity shows a bend at around 0.6 N load for (001). A slight bending of this type is also observed at around 0.7 N load for (110). This could be attributed to the fact that the cracks become prominent for indents of higher loads (>0.6 N) and that transition from a Palmqvist to median crack system also occurs at higher loads as has also been observed and interpreted in other systems [15, 16].

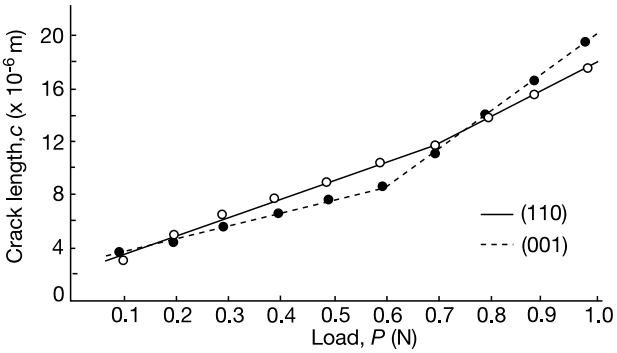

Figure 3. Dependence of crack length on load for the two planes.

Using the relation $B_i = H_v/K_c$ given by Nihara *et al* [13], the average values of brittleness index B_i for (110) and (001) planes are calculated as 6.25×10^3 and 6.11×10^3 m$^{-1/2}$ respectively for loads $P \geqslant 0.8$ N only.

3.3. Hardness anisotropy

In order to study the anisotropy exhibited by (110) and (001) planes of $GdAlO_3$ crystals, directional hardness was determined by rotation of the indenter over a range of 0–180° in steps of 15°. The initial position (0°) was taken when one of the diagonals of the indenter on the (110) plane was parallel to the ⟨001⟩ direction. The same applies to the measurements on the (001) plane. A load of 0.49 N was chosen in order to obtain the optimum size of the indentation mark.

Figure 4 shows the variation of microhardness values with orientation of the indenter. From the graph, the following points emerge.

(1) Whether the plane considered is (110) or (001), the variation is periodic, the maxima and minima repeating after every 30° change in orientation.

(2) The minima of the (110) plane correspond to the maxima of the (001) plane and vice versa.

(3) The ratio between the two extreme values of hardness i.e. $H_v(\max)/H_v(\min)$ is 1.133 and 1.116 for (110) and (001) planes respectively.

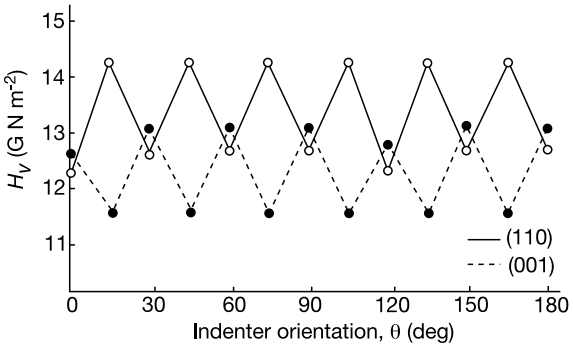

Figure 4. Variation of H_v with indenter orientation.

The hardness anisotropy observed here is attributed to the effective resolved shear stress on the slip system operating in the crystal as has been reported for other crystals, *viz*., CaF_2 [17], Zn and silicon ferrites [18], InP [19], NaCl [20], rubidium halides [21], InSb and III–V compounds [22, 23] and perovskite structures of the type $RFeO_3$ (R = Er, Yb, Dy, Y) [15, 24, 25]. The observed hardness anisotropy has been attributed to the effective resolved shear stress (ERSS) developed beneath the indenter and hence to the active slip systems operating in the crystals on application of stress [15, 17, 24–27]. Since the measuring instrument, the Vickers indenter, has fourfold symmetry which repeats the value of H_v after every 90° rotation, it is expected that there would be a manifestation of threefold symmetry as far as the anisotropy property of microhardness of the crystal is concerned. It has been observed that $H_v(110) > H_v(001)$. In such a case, anisotropy coefficient A is defined as

$$A = \Delta H_v / H_v(110)$$

where $\Delta H_v = H_v(110) - H_v(001)$.

The average value of A comes out to be 0.129 for the crystal.

3.4. Dielectric studies

The variation of dielectric constant ϵ' and dielectric loss ($\tan\delta$) of the $GdAlO_3$ crystal is studied at room temperature (20 °C) as well as at higher temperatures up to 210 °C in the frequency range of 1 kHz to 13 MHz. Conductivity variations with temperature at different frequencies of the applied a.c. field are also studied. The results are discussed below.

The dependence of dielectric constant (ϵ') and dielectric loss ($\tan\delta$) on frequency of the applied a.c. field at different temperatures is shown in figures 5 and 6. Figures 7 and 8 show the dependence of dielectric loss ($\tan\delta$) and conductivity (σ) on temperature at different frequencies. These curves suggest that the dielectric constant and dielectric loss are strongly dependent on temperature and frequency of the applied a.c. field. This type of behaviour is common in the case of ionic systems [28, 29]. The conductivity is found to be more at higher frequencies and this has been observed in other materials [29–31]. The increased conductivity could be due to reduction in space charge polarization at higher frequencies [32].

Figure 9 shows the plots of dielectric constant against temperature at different frequencies (1, 5 and 10 MHz) of the applied a.c. field. The curves reveal the following points:

(1) There is almost a linear rise in dielectric constant up to a temperature of 90 °C at all the three frequencies considered (i.e. 1, 5 and 10 MHz). Between 110 and 170 °C, ϵ' remains almost independent of temperature.

(2) After 170 °C, ϵ' shows a fall in its value and this behaviour is seen at all the frequencies considered. This anomalous behaviour of ϵ' against temperature suggests some transition taking place at 170 °C.

The curves of figure 7 suggest that there is smearing of the transition which remains practically independent of frequency in the range 1 MHz–10 MHz. The term diffuse phase transition was coined in the early literature to describe the smeared responses but it is now realized that there may not be a genuine thermodynamic phase transition in these systems with smeared response and it may, therefore, be better called simply a diffuse/smeared transition.

It was shown by Smolensky and Isupov [33] that solid solutions of $BaTiO_3$ perovskite with large concentration of $BaSnO_3$ do not exhibit the usual sharp change in dielectric constant at T_c characteristic of the ferroelectric transition in $BaTiO_3$. Instead, the dielectric response is smeared out. Several other solid solutions as well as complex compounds with perovskite and tungsten bronze structures have been discovered where the dielectric constant versus temperature plots exhibit broad humps. One of the common characteristics of all these materials is the existence of different cations at the equivalent crystallographic positions in the unit cell [34]. Prominent perovskite systems exhibiting smeared out dielectric response are classified as

(i) isovalent substitutional solid solutions,
(ii) offvalent substitutional solid solutions and
(iii) complex perovskite compounds with order–disorder at the B site.

The role of compositional inhomogeneities and particle size in the context of diffuse transitions in $BaTiO_3$ based systems has been discussed by Pandey [34]. Broadening or diffuseness in the transition of Dy doped barium sodium niobate ceramics has been attributed to compositional fluctuation caused by the doping of Dy [35] and analogous to certain compounds with perovskite structure [36]. The smeared/diffuse transition in the case of $GdAlO_3$ as observed in figure 9 spread over a temperature range of about 110–170 °C at

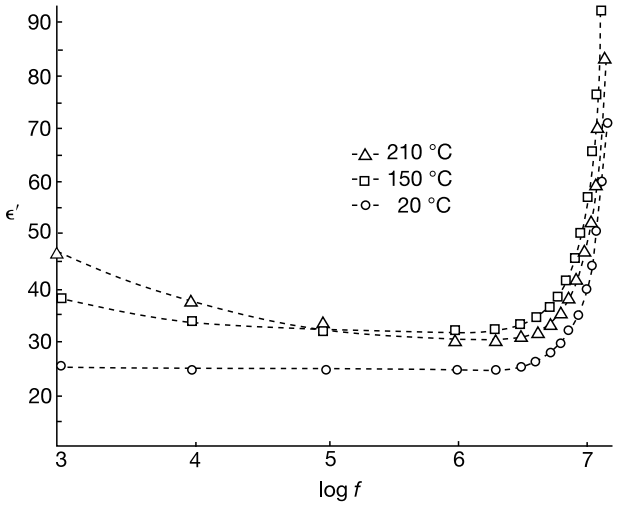

Figure 5. Dependence of dielectric constant ϵ' on frequency at 20, 150 and 210 °C.

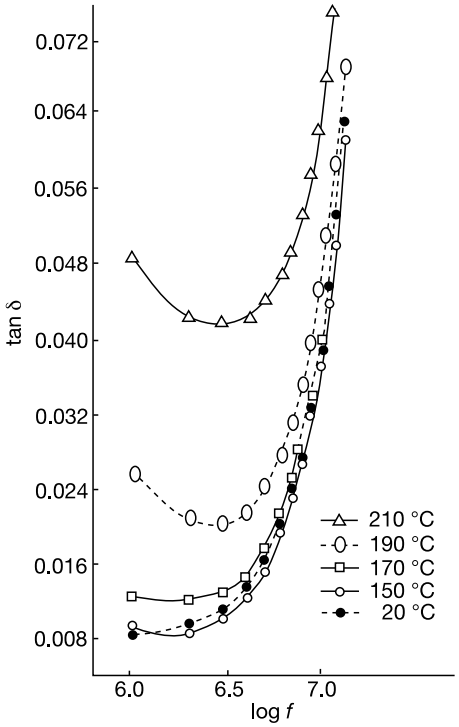

Figure 6. Dependence of dielectric loss ($\tan\delta$) on frequency at 20, 150, 170, 190 and 210 °C.

almost all the frequencies is attributed to the entrance of lead into the structure. $GdAlO_3$ crystals grown from $PbO/PbF_2/B_2O_3$ flux have been reported to contain 0.3% Pb [6]. Kotru [37] has also reported that secondary crystallization of $PbAl_{12}O_{19}$ and Pb_2OF_2 occurs during the growth of $RAlO_3$ resulting in inhomogeneity in the crystals. Pb^{2+} derived from the flux replaces the rare-earth ion R^{3+} of the crystals of $RAlO_3$ resulting in the formation of

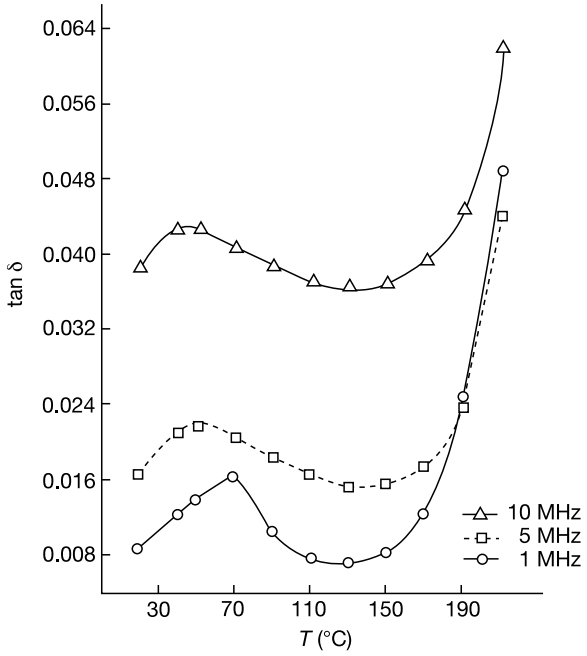

Figure 7. Dependence of dielectric loss ($\tan\delta$) on temperature at 1, 5 and 10 MHz frequencies.

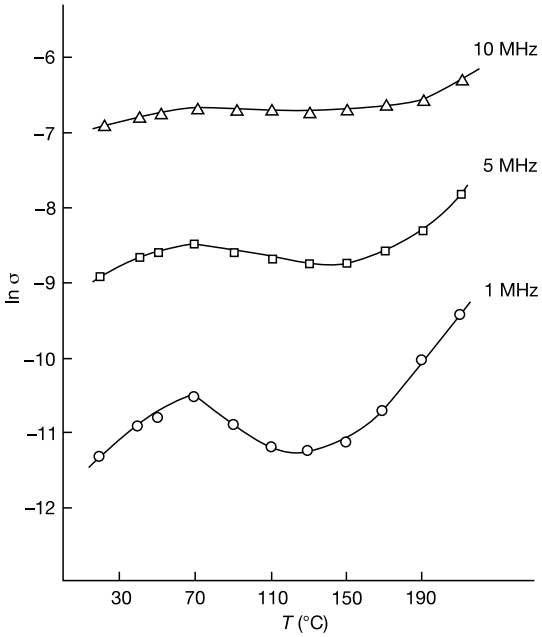

Figure 8. Variation of conductivity (σ) with temperature at different frequencies.

$PbAl_{12}O_{19}$. The formation of secondary/impurity phases and their entry into $RAlO_3$ crystals as inclusions causes inhomogeneity of the $RAlO_3$ crystal [37, 38]. It is thus conjectured

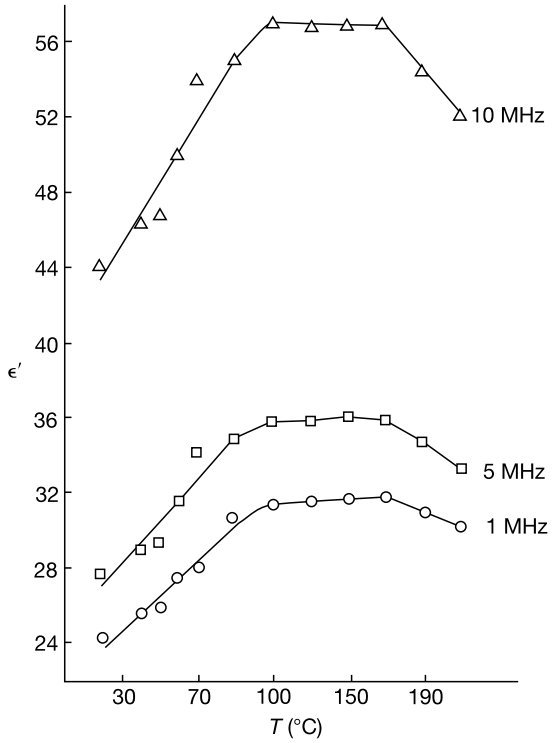

Figure 9. Plots of dielectric constant ϵ' against temperature at 1, 5 and 10 MHz frequencies.

that the smeared/diffuse transition in $GdAlO_3$ as observed in figure 9 may be due to the inhomogeneity caused by the offvalent substitution of foreign ions or impurities.

It would have been interesting to study changes in the microhardness values and the corresponding mechanical parameters that may be brought about at the transition temperature (170 °C), but due to non-availability of an *in situ* high-temperature microhardness measuring device, it was not possible to do so at this stage.

4. Conclusions

(1) The average values of Vickers hardness number of flux-grown $GdAlO_3$ crystals are 13.59 and 11.83 GN m^{-2} for (110) and (001) planes respectively.

(2) The variation of microhardness with load is non-linear for both the planes and can be better explained by the law of material resistance pressure of Hays and Kendall. Load independent values of hardness are $H_v(110) = 12.23$ GN m^{-2} and $H_v(001) = 11.08$ GN m^{-2}.

(3) The average values of fracture toughness and brittleness index as calculated for median cracks turn out to be 2.06, 1.87 MN $m^{-3/2}$ and 6.25×10^3, 6.11×10^3 $m^{-1/2}$ for the (110) and (001) planes respectively.

(4) The hardness anisotropy is reflected by the periodic variation of H_v with respect to the orientation of the indenter, the maxima and minima being repeated after every 30° change in orientation.

(5) The dielectric constant versus temperature curves suggest some transition taking place at 170 °C, both dielectric constant ϵ' and dielectric loss ($\tan\delta$) being strongly dependent on temperature and frequency of the applied a.c. field.

(6) The conductivity increases with temperature until 70 °C, decreases thereafter until 130 °C and then again increases, its value being more at higher frequencies. The increase in the value of conductivity may be due to reduction in space-charge polarization at higher frequencies.

(7) The transition in $GdAlO_3$ is the smeared/diffuse type which may be due to inhomogeneity caused by the offvalent substitution of foreign ions or impurities.

References

[1] Cashion J D, Cooke A H, Hawkes J F B, Leask M J M, Thorp T L and Wells M R 1968 *J. Appl. Phys.* **39** 1300
[2] Cashion J D, Cooke A H, Leask M J M, Thorp T L and Wells M R 1968 *J. Mater. Sci.* **3** 402
[3] Shaji Kumar M D, Srinivasan T M and Ramaswamy P 1994 *8th Natl Semin. on Ferroelectrics and Dielectrics* (Nagpur, 1994)
[4] Adak A K, Ghosh B B and Pramanik P 1996 *9th Natl Semin. on Ferroelectrics and Dielectrics* (New Delhi, 1996)
[5] Kotru P N, Razdan A K and Wanklyn B M 1989 *J. Mater. Sci.* **24** 793
[6] Wanklyn B M 1969 *J. Cryst. Growth* **5** 323
[7] Geller S and Bala V B 1956 *Acta. Crystallogr.* **9** 1019
[8] Mott B W 1966 *Microindentation Hardness Testing* (London: Butterworths) p 9
[9] Pandya J R, Bhagia L J and Shah A J 1983 *Bull. Mater. Sci.* **5** 79
[10] Brookes C A 1986 *2nd Int. Conf. on Science of Hard Materials (Rhodes)* (*Inst. Phys. Conf. Ser. 75*) (Bristol: Hilger) ch 3
[11] Kick F 1885 *Das Gesetz der propertionalen Widerstande and Seine Anwendung, Delidzig (Felix 1885)*
[12] Hays C and Kendall E G 1973 *Metallography* **6** 275
[13] Nihara K, Movena R and Hasselman D P H 1982 *J. Mater. Sci. Lett.* **1** 13
[14] Lawn B R and Fuller E R 1975 *J. Mater. Sci.* **9** 2016
[15] Sharma K K, Kotru P N and Wanklyn B M 1994 *Appl. Surf. Sci.* **81** 251
[16] Beigh Shafqat, Kotru P N and Wanklyn B M 1995 *Mat. Chem. Phys.* **40** 99–104
[17] Brookes C A and Burnand R P 1973 *Science of Hardness Testing* ed J H Westbrook and H Conrad (Metals Park, OH: American Society for Metals) p 199
[18] Wytt R 1974 *Metals, Ceramics and Polymers (London, 1974)* ch 5, 6
[19] Brasen D 1976 *J. Mater. Sci.* **11** 791
[20] O'Neill J B 1970 *PhD Diss.* University of Bradford
[21] Thirmal Rao T and Sirdeshmukh D B 1991 *Cryst. Res. Technol.* **26** 3
[22] Lange V N and Lange T I 1963 *Fiz. Tverd. Tela* **5** 2029
[23] Willardson R K and Beer A C 1968 *Physics of III–V Compounds (Semiconductor and Semimetals 4)* (New York: Academic)
[24] Raina U, Bhat S, Wanklyn B M and Kotru P N 1993 *Mater. Chem. Phys.* **34** 257
[25] Bamzai K, Kotru P N and Wanklyn B M 1996 *Cryst. Res. Technol.* **31** 813
[26] Bhatt V P, Patel R M and Desai C F 1983 *Cryst. Res. Technol.* **18** 1173
[27] Bhatt V P, Desai C F and Shah R C 1983 *Res. Mech.* **9** 35
[28] Rao K V and Smakula A 1965 *J. Appl. Phys.* **36** 2031
[29] Rao K V and Smakula S 1966 *J. Appl. Phys.* **37** 319
[30] Lokanatha S and Bhattacherjee S 1984 *J. Mater. Sci. Lett.* **3** 299
[31] Gon H B and Rao K V 1980 *Ind. J. Phys.* **54A** 50
[32] Jonscher K 1989 *J. Mater. Sci.* **24** 372
[33] Smolensky G A and Isupov V A 1954 *Zh. Tekh. Fiz.* **24** 1375
[34] Pandey D 1995 *Diffusionless Phase Transitions in Oxides* ed C Boulesteix (Trans Tech) pp 177–216
[35] Subha Rao P S V and Sambasiva Rao K 1990 *Ferroelectrics* **102** 183–90
[36] Smolensky G A, Isupov V A, Agranovskya A I and Popov S N 1960 *Sov. Phys.–Solid State* **2** 2584
[37] Kotru P N 1996 *Natl Semin. on Ferroelectrics and Dielectrics* (New Delhi, 1996)
[38] Razdan A K 1989 *PhD Thesis* Jammu University